DEVELOPMENT OF NEUTRON COUNTER FOR MEASURING β-DELAYED NEUTRON DECAY IN r-PROCESS NUCLEI

P. Santi[a], P.T. Hosmer[a], D. Hale, K.-L. Kratz[b], B. Pfeiffer[b], P.L. Reeder[c], H. Schatz[a]

The r process is one of the major nucleosynthesis processes in the universe producing roughly half of all elements heavier than iron. While the overall processing mechanism of the r process is generally known as a series of rapid neutron captures and β-decays, one of the biggest problems in nuclear astrophysics remains the question of the astrophysical site of the r process. In order to identify the site of the r process, it is necessary to quantitatively understand the r process so as to interpret the new data on r process enriched metal poor stars expected from programs at observatories world wide. One crucial piece of data that is needed in performing these r process calculations are the branchings for β-delayed neutron emission P_n between the r process path and stability, which are especially important as they can produce similar effects as neutrino post processing. In order to measure the β delayed neutron emission branching of r process nuclei, a new neutron detector is being developed at the NSCL capable of measuring low energy neutrons, ranging from 1 keV to approximately 6 MeV, that are typically emitted from β-delayed neutron decay.

There are several methods for detecting neutrons, depending on the characteristic energy range of the neutrons. In detecting β-delayed neutrons, proportional counters have been used before to successfully determine the neutron emission probabilities for light neutron rich nuclei around ^{25}F by Reeder, et al. [1] as well as r process nuclei using the Mainz 4π detector [2, 3, 4]. These proportional counters contain a gas such as ^{3}He or BF_3 which has a high (n,p) or (n,α) capture cross section for neutrons at thermal energies. Since the neutrons emitted in conjunction with β decay are not thermalized, the proportional counters are placed in a material to moderate the neutron energy in order to maximize the probability of detecting the neutrons. The performance of a detector which uses this technique depends critically upon the configuration of the proportional counters within the moderating matrix, as well as the properties of the moderating material itself. Many various configurations of proportional counters and moderating materials have been used in previous experiments (e.g. [5, 6, 7, 8]).

In determining an optimal configuration for our detector, several experimental criteria were considered. A large detection efficiency is required due to the low intensities which are expected from the Coupled Cyclotron Facility for the neutron rich nuclei of interest. Furthermore, a relatively flat efficiency curve over the whole energy range of interest is required to minimize the uncertainties in determining the neutron emission probabilities since the energies of the neutrons are not directly measured because of the moderation. Shielding against background neutrons, for example from fragmentation reactions of the fast radioactive beams with material in the beamline, is also and important consideration. Finally, the detector must be designed to work in conjunction with the existing NSCL β-decay end station, and utilize existing proportional counters at collaborating institutions.

To optimize the detector design in meeting these criteria, the code MCNP (Monte Carlo N-particle) [9] was used to simulate the transport of the neutrons through the detector. MCNP has been used successfully in simulating the performance of other neutron detectors [1, 10]. From these simulations, it was clear that the configuration which best suited the experimental needs was one in which the proportional counters were placed in concentric rings surrounding the implantation chamber, as had been done with the 4π detector [11], and by Reeder, et al. [1, 12]. This arrangement gives a relatively high efficiency for a large range of energies, and also allows for the extraction of some neutron energy information based on the distribution of events among the concentric circles [13]. The simulations also showed that in order to achieve a high detection efficiency which did not vary as a function of the neutron energy, a complex balance had to be achieved between the amount of detector gas and the amount of moderating material in the counter. For instance, the simulations revealed that a minimum amount of moderator surrounding each proportional counter in the detector is necessary in order to maximize the probability that the neutron would scatter off of the dense moderating material and pass through the proportional counter. The simulations also showed that in order to maximize the detection of higher energy

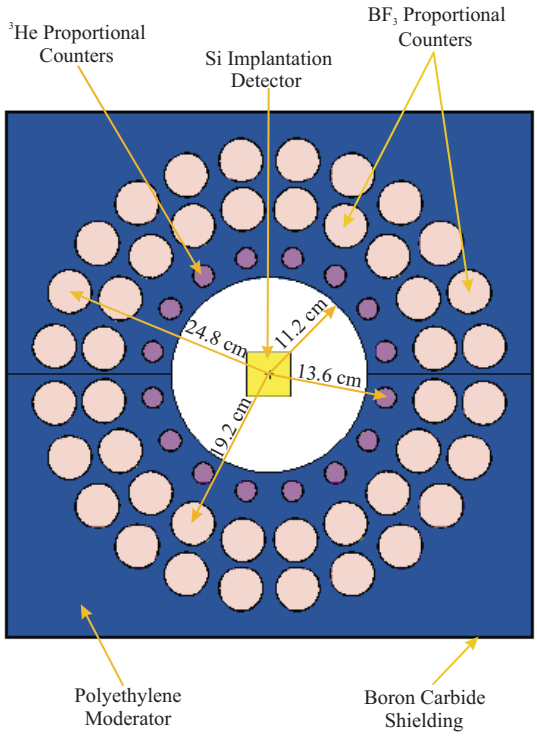

Figure 1: Schematic drawing of the neutron detector.

neutrons, the locations of a outer rings relative to the implantation detector had to be carefully considered in order to balance neutron moderation with neutron capture in the moderator. Finally, in order produce as flat an efficiency curve as possible, it is was determined that the spacing between rings is crucial in order to have each ring of proportional counters measure different ranges of neutron energies. To optimize the design with respect to these various effects, the following parameters were considered in the MCNP simulations: the number of rings of proportional counters, the spacing between the rings, the number of counters in each ring, and the amount of moderating material beyond the outer ring.

The final design of the detector is shown in Figure 1. It consists of a moderating block 60 cm by 60 cm by 80 cm, containing three concentric rings of proportional counters. The detector possess 60 proportional counters with 16 ^{3}He counters in the inner ring, 20 Boron Trifluoride (BF_3) counters in the middle ring, and 24 BF_3 counters in the outer ring. The beam line hole is designed large enough to contain the existing β-decay end station. Surrounding the moderator is a layer of boron carbide for absorption of background neutrons, as well as a 3/4 inch Aluminum case for handling. During the experiment, an additional foot of paraffin will be placed around the detector to moderate the background neutrons in order to maximize the possibility of these neutrons being captured in either the paraffin or boron carbide layers. The thick layer of paraffin reduces the amount of background neutron flux that is measured in the detector by about a factor of 10^{-6} for neutron energies less than 100 keV based on the results of MCNP simulations shown in Figure 2. With the placement of the Boron Carbide layer between the paraffin shielding and the polyethylene moderator in the detector, the upper limit of the neutron energy range for which a shielding factor of $< 10^{-6}$ is achieved is extended from 100 keV to 600 keV due to the large capture cross section of ^{10}B at low neutron energies. A slight increase of approximately 100 keV to this upper limit of the background neutron energy can be achieved if one substitutes a 2 mm Cadmium layer for the 8 mm Boron Carbide absorption layer. While the effectiveness of the shielding does gradually decreases with an increase in neutron energy, the shielding combination of Paraffin and Boron Carbide still reduces the

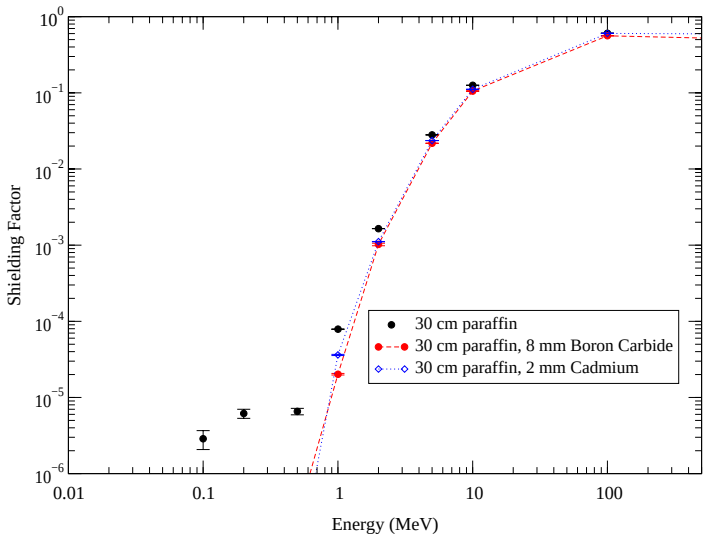

Figure 2: Ratio of number of background neutrons detected with shielding to the number of neutrons detected without shielding as a function of neutron energy based on MCNP simulations for various shielding combinations. The MCNP simulations assumed a parallel beam of monoenergetic neutrons from a source 20 cm x 20 cm in area, which was placed 140 cm away from a side of the detector. The lines in the figure are to guide the eye.

background neutron flux that is detected by a factor of 10 for neutron energies around 10 MeV.

In Figure 3, the calculated detection efficiency is plotted for this detector as a function of neutron energy. As can be seen in the figure, the efficiency curve is relatively constant at 45% from 1keV to 500 keV, dropping off to around 26% by 5 MeV. This drop off in efficiency at larger energies is due to the fact that as the neutrons transverse more of the polyethylene, the probability of neutron capture by hydrogen atoms in the polyethylene via the (n,γ) capture reaction increases as well. While the drop off in detector efficiency at larger neutron energies is common in neutron detectors which use polyethylene as a moderator, the rate at which the drop off occurs can vary depending on the specific placement of the neutron counters. In Table 1, the characteristics of the current neutron detector are compared with the 4π detector [11] and the Reeder detector [1] in terms of the maximum efficiency achieved ϵ_{max}, the relative variation in the efficiency from the maximum value for $E_n < 1$ MeV $\Delta\epsilon$, and the neutron energies at which the efficiency varies by 20% and 40% relative to the maximum efficiency, based on MCNP simulations of the three detector systems. As can be seen in Table 1, most of the characteristics of the current detector are similar to the characteristics of the detector developed by Reeder, et al [1] and the 4π detector [11] with the only exception being a lower ϵ_{max} than was achieved in the Reeder detector. This difference between the Reeder detector and the current design is understandable considering the fact that the proportional counters in the current design are much further away from the neutron source than the Reeder detector due to a beam hole that is 5 times larger than the hole in the Reeder detector (see Table 1). The fact that the beam hole size for the current design is so much bigger than the other two detectors and yet maintains a relatively high ϵ_{max} with a small variation in the detection efficiency is quite remarkable. This small variation in detection efficiency was achieved by adjusting the specifics of each ring (location of the ring relative to the implantation detector as well as number of detectors in each ring) so that each ring reached a maximum efficiency at different neutron energies.

As of this report, the moderating block is currently under construction at the NSCL. Once the detector has been completed and assembled, a calibration experiment will be performed at the University of Notre Dame using (p,n) reactions to produce nearly mono-energetic neutrons in order to measure the efficiency of the detector as a function of neutron energy, similar to what was done in Ref. [14]. The first experiment using the detector

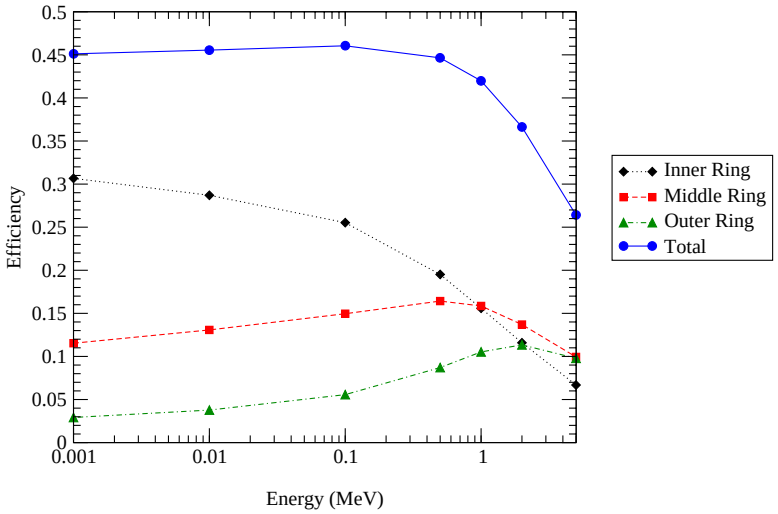

Figure 3: Neutron detection efficiency for the neutron counter as a function of initial neutron energy as calculated using MCNP. The lines in the figure are to guide the eye.

Table 1: Comparison between the characteristics of the current neutron detector, the Reeder detector, and the Mainz 4π detector based on MCNP simulations of the three detectors.

Detector	Beam Hole Radius (cm)	ϵ_{max}	$\Delta\epsilon$ ($E_n < 1$ MeV)	20% variation limit (MeV)	40% variation limit (MeV)
Reeder, et al.	2.6	64%*	9.2%	2.0 MeV	4.7 MeV
Mainz 4π	5.5	44%	11.67%	1.8 MeV	4.0 MeV
NSCL detector	11.2	46 %	8.6%	2.0 MeV	4.6 MeV

* Data taken from Ref. [1]

will then be performed at the NSCL to study the β decay half lives and β-delayed neutron emission probabilities of neutron rich isotopes in order to understand the 'weak' component of the r-process.

a: NSCL, Michigan State University, East Lansing, MI 48824, USA
b: Institut für Kernchemie, Universität Mainz, D-55099 Mainz, Germany
c: Pacific Northwest National Laboratory, Richland, WA, 99352

References

1. P.L Reeder *et al.*, Phys. Rev. C **44**, 1435 (1991).
2. T. Mehren *et al.*, Phys. Rev. Lett. **77**, 458 (1996).
3. J.C. Wang *et al.*, Phys. Lett. B **454**, 1 (1999).
4. M. Hannawald *et al.*, Phys. Rev. C **62**, 054301 (2000).
5. R.L Macklin and J.H. Gibbons, Phys. Rev. **109**, 105 (1958).
6. R.F. Barrett, J.R. Birkelund, and H.H. Thies, Nucl. Instrum. Methods Phys. Res. **68**, 277 (1969).
7. L.V. East and R.B. Walton, Nucl. Instrum. Methods Phys. Res. **72**, 161 (1969).
8. K.K. Sekharan, H. Laumer, B.D. Kern, and F. Gabbard, Nucl. Instrum. Methods Phys. Res. **133**, 253 (1976).
9. J.F. Briesmeister, computer code MCNP, version 4a, Los Alamos National Laboratory Report No. LA-12625-M (1993).
10. P.R. Wrean and R.W. Kavanagh, Phys. Rev. C **62**, 055805 (2000).
11. O. Sorlin *et al.*, Nucl. Phys. A **583**, 763 (1995).
12. P.L. Reeder and R.A. Warner, Nucl. Instrum. Methods Phys. Res. **180**, 173 (1981).

13. J.T. Caldwell, R.L. Bramblett, B.L. Berman, R.R. Harvey, and S.C. Fultz, Phys. Rev. Lett. **15**, 976 (1965).
14. E. Lund, P. Hoff, K. Aleklett, O. Glouset, and G. Rudstam, Z. Phys. A **294**, 233 (1980).